A Dissipation-Based Method for Improving the Accuracy of Computational Fluid Dynamics Simulations of High Level Non-Newtonian Waste - 17351

Ahmadreza Abbasi Baharanchi*, Seckin Gokaltun*, Dwayne McDaniel*
*Applied Research Center, Florida International University
10555 W Flagler St., EC2100, Miami, FL 33174

ABSTRACT

Analysis of shear rate in dissipative scales of turbulence was performed using a quasi-direct numerical simulation (Q-DNS) of flow through a pipe involving Bingham fluid. Dependency of deformation rate on dissipative scales of turbulence was studied and a modification algorithm was developed and implemented in Reynolds-averaged Navier-Stokes (RANS) modeling of the same flow using the standard k-ε model. It was shown that the modification was effective in increasing accuracy of the RANS simulations when the velocity profile was modified to match experimental data. In both the Q-DNS and RANS simulations, the Herschel-Bulkley (HB) rheology equation was used to relate shear stress of the non-Newtonian fluid to shear deformation. Additional analysis of dependency of shear on the turbulent dissipation rate (TDR) was performed using various flow conditions in RANS simulations with a modified viscosity model (alpha model). In the past, the alpha model has been shown to produce accurate simulations for the same flow conditions. Results of the analysis shows that a qualitative agreement exists between shear dependency in the RANS-alpha and Q-DNS-HB simulations when the ratio of velocity to length scale is used.

INTRODUCTION

Accurate simulation of flow systems involving non-Newtonian fluids such as waste processing systems in the US Department of Energy's sites has attained a great deal of attention. Computational fluid dynamics (CFD) can play a significant role in assisting engineers to safely and optimally transfer the waste from single shell tanks to double shell tanks [1,2]. CFD simulations can be validated by experiments and run with different types of simulants that can be used for further predictions. According to [3] variable particle concentration in simulants can cause variation of viscosity and simulant is then considered to be a non-Newtonian fluid. Laponite-based simulants with concentrations approximately 1.5 wt% was used in experimental and simulation studies by [4-6], respectively. Shear stress in this simulant varies according to Bingham fluid characteristics [7] and can be modeled using Herschel–Bulkley rheological model [8].

The literature contains valuable efforts that seek to improve accuracy of numerical algorithms in the prediction of flow characteristics of non-Newtonian fluids. Wilson and Thomas [9] improved the theory of the Power-law and Bingham plastic fluids for the log-law region of the velocity profile towards better prediction of the wall friction coefficient. Their analysis was based on drag reduction associated with non-Newtonian fluids and colloidal suspensions, as was first reported by [10], according to [11]. This modification resulted in enhanced viscosity effects for dissipative

micro-eddies that possess small time and length scales. Soto and Shah [12] developed an algorithm for simulation of an entrance flow of a yield-power-law fluid, which produced results in good agreement with analytical solutions for different yield stress and power-law exponents. Bartosik [13] applied a theory by [9], which described a change of boundary layer thickness and suppression of turbulence in the boundary layer for slurry flow with very fine solid particles. Bartosik employed a k-ε turbulence model with modified damping functions and compared the performance of the power-law and Herschel and Bulkley [8] models in the simulation of Kaolin slurry. He found that the later model can better describe shear stress at a low shear deformation rate.

Despite these significant contributions, there is still a need to find a universal model to define viscosity properly in an entire computational domain for different regimes of flow so that its applicability is not specific to a flow with certain material, geometry, and boundary conditions. One possible approach is to dynamically modify the viscosity during the simulation. In this study, two different approaches of achieving this goal were implemented. In the first approach, parameters, such as shear rate, that affect the viscosity were modified. This approach was pursued by researchers including [14] and [6] who designed a method to alter viscosity by correcting the definition of shear rate. In the second approach the viscosity is directly altered following a specific algorithm. Baharanchi et al. [15] introduced a direct viscosity adjustment method, called the alpha method, that can modify viscosity in the domain based on the dissipation rate of the kinetic turbulent energy and dynamically reconstructed rheogram of a non-Newtonian fluid. Their method, known as the alpha method, was effective in improving results of Reynolds Averaging Navier-Stokes (RANS)-HB simulations for laminar, transitional, and turbulent flows.

in this research, previously reported simulation results from the RANS-alpha method were considered for the shear dependency analysis. Additional simulations using the RANS-alpha method were conducted as an extension of our investigations and a similar shear analysis was conducted. The RANS simulations were based on the standard k-ε turbulence model and a modified HB-based viscosity model (alpha model). Later, shear dependency analysis of the most recent results obtained from a quasi-direct numerical simulation (Q-DNS) was considered. Results of this analysis were used as a baseline to find relationships for the shear rate in dissipative scales of turbulence. Finally, relationships obtained from Q-DNS simulations for shear rate were incorporated into a RANS-HB simulation according to an algorithm that was developed for alteration of the shear rate for a Reynolds number of 25,300. We compared shear rate variations between Q-DNS-HB and RANS-alpha simulations to evaluate similarities. Finally, correlations obtained from Q-DNS were implemented into the RANS-HB method to investigate possible improvements.

SIMULATIONS

Dependency of Shear Rate on Dissipative Scales

Shear rate plays a critical role in simulation studies of non-Newtonian fluids. Direct dependency of viscosity on the shear rate is a fundamental characteristic of non-Newtonian fluids. Analysis from [14] showed that there is a strong dependency between shear rate and dissipation rate of turbulent kinetic energy. This dependency can be obtained from a direct numerical simulation (DNS) or a large eddy simulation (LES) where shear is calculated based on gradients of instantaneous velocity components. In addition, it is interesting to observe this dependency in a RANS simulation which accurately predicts the velocity field and compare it to results from the DNS simulation. Research efforts may look for possible approximations if deviations are not significant. Therefore, an analysis was performed for results obtained previously from both the RANS-alpha and Q-DNS-HB simulations. In this analysis, variation of the shear rate against a quantity defined by Equation (1) was obtained for dissipative scales. u_{rms} and η represent velocity and length scale of turbulent scales. In this equation K, υ, and ε, represent turbulent kinetic energy (TKE), kinematic viscosity, and TDR, respectively. This quantity has the same units of shear rate, sec^{-1}, and is zero for non-dissipative scales. In the case where the average value of ε is obtained from spatial analysis, η will then represent Kolmogorov length scale, which is the smallest scale in turbulent flow. In RANS, K and ε are obtained from the solution to the closure equations of TKE and TDR and are directly accessible from STAR-CCM+. In Q-DNS, TKE and TDR must be obtained from fluctuations of velocity components. For this purpose, direct definition of u_{rms} and TDR are obtained from Equation (2) and Equation (3).

$$\frac{u_{rms}}{\eta} = \frac{\sqrt{\frac{2K}{3}}}{\frac{\upsilon^{3/4}}{\varepsilon^{1/4}}} \qquad \text{(Eq. 1)}$$

$$u_{rms} = \sqrt{\frac{1}{3}(u_{x,rms}{}^2 + u_{y,rms}{}^2 + u_{z,rms}{}^2)}, \quad u_{x,rms} = \sqrt{\overline{\acute{u}_x{}^2}}, \quad u_{y,rms} = \sqrt{\overline{\acute{u}_y{}^2}}, \; u_{z,rms} = \sqrt{\overline{\acute{u}_z{}^2}} \qquad \text{(Eq. 2)}$$

$$\varepsilon = \mu \left(2\overline{\frac{\delta \acute{u}_x}{\delta x}^2} + 2\overline{\frac{\delta \acute{u}_y}{\delta y}^2} + 2\overline{\frac{\delta \acute{u}_z}{\delta k}^2} + \overline{\left(\frac{\delta \acute{u}_x}{\delta y} + \frac{\delta \acute{u}_y}{\delta x}\right)^2} + \overline{\left(\frac{\delta \acute{u}_x}{\delta z} + \frac{\delta \acute{u}_z}{\delta x}\right)^2} + \overline{\left(\frac{\delta \acute{u}_y}{\delta z} + \frac{\delta \acute{u}_z}{\delta y}\right)^2}\right) \qquad \text{(Eq. 3)}$$

In RANS, this analysis was performed on results obtained from RANS-alpha method. Additional analysis was also performed for flow in turbulent regimes (Re = 10000, 15000, and 20000) to observe similarities between profiles. Results as shown in Figure 1(a), demonstrate similar profiles that are non-linear and increase and shift to the right with increasing Reynolds number. This is a result of higher shear and velocity rms in higher Reynolds numbers. In addition, each profile has a comparable maximum shear rate and maximum u_{rms}/η and perhaps normalization of the results can make all profiles coincide. Additional and similar analysis was

performed using the ratio of turbulent dissipations to turbulent kinetic energy, which has the same units as of shear rate (1/sec). For each Reynolds number shown in Figure 1(b), a profile with small slope is preceded with a profile having a significantly larger slope. The former is indicative of variations in the vicinity to solid boundaries and the slope of this profile grows with increasing Reynolds number. In contrast, variations with almost equal slopes are observed in small values of TDR/TKE for different Reynolds numbers. Similarity between these profiles suggest that a correlation can be obtained and implemented into the RANS-HB modeling to directly modify the shear rate based on TDR/TKE values.

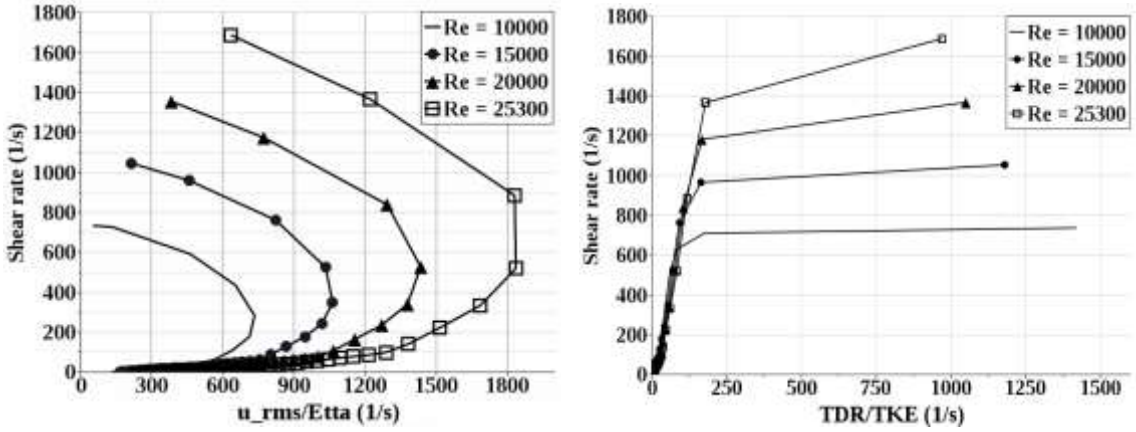

Fig. 1. Variation of Shear Rate versus Different Ratios.

Analysis of Shear Using Q-DNS Simulation

Detailed study of turbulent flows requires access to information involving all ranges of velocity and length scales that exist in the flow. Direct numerical simulation (DNS) is the most widely accepted benchmark tool that can provide invaluable information for dissipative and non-dissipative structures of fluid flows. A quasi-DNS solver is less stringent in spatial and temporal discretization requirements compared to DNS solver and can still simulate the flow with exceptional accuracy ([16-19]). More details about this solver is available from [19]. A DNS solver is available in STAR-CCM+ through use of the Large Eddy Simulation solver with an extremely small filter size. This solver uses a second order central scheme with 5% boundedness (for space discretization) in combination with a second order implicit scheme (for time integration). Schemes and the simulation set up are summarized in Table 1. For quicker and more accurate analysis, a two-dimensional profile of velocity measured by [4] was reconstructed in three dimensions and assigned to the inlet boundary condition. Profiles of the velocity was obtained at the outlet of the computational domain and was averaged over 7.5 seconds of flow physical time to ensure that good agreement was obtained with the experimental profile.

TABLE I. Boundary Conditions, Geometry and Fluid Properties in RANS Simulations

Boundary, Geometry, and Mesh Conditions			
B.C. (case: RE =25300)		**Mesh**	
Inlet velocity, v_i (m/s)	2.03	$N_R \times N_\Theta \times N_Z$	110×88×100
Mass flow rate, $\dot{m}$ (kg/s)	15.94	$\Delta r+$, $\Delta_\Theta+$, $\Delta z+$	0.1 →26
Pressure at outlet	1atm	Courant number	1.5
wall	Non-slip	Y+	0.05
Fluid properties		**Pipe dimensions**	
Density, $\rho(kg/m^3)$	1000	Length (m)	0.25
Yield stress, τ_y (pa)	4.42	Diameter (m)	0.1
Consistency factor, k ($Pa.s^n$)	0.242	Number of prism layer	20
Exponent, n	0.534	Mesh (Polyhedral + Hexahedral)	

Figure 2Fig. 2(a) shows the contour of the axial velocity along the pipe obtained from a Q-DNS simulation of pipe flow at T = 7.5 seconds. We compared the averaged velocity on a probe at the outlet with experimental data available in the literature. Figure 2(b) shows that a very good agreement exists between simulation and experimental results. In addition, velocity magnitude and turbulent dissipation rates are shown for various structures of turbulence obtained from iso-surfaces of Q-criterion in Figure 2(c-d).

To better separate regions of low and high dissipation, the maximum value on the scale was set to 0.1, which shows strong dissipation occurring at walls of the domain. Next, we continued the same analysis of shear rate which was performed for results of the RANS-alpha method. Variation of shear rate versus u_{rms}/η and TDR/TKE were obtained and plotted for turbulent structures, as shown in Figure 3(a-b). TDR was calculated from Equation 3 and TKE = $0.5*(\acute{u}_x^2+\acute{u}_y^2+\acute{u}_z^2)$. Figure 3(a) shows that a qualitative similarity exists between Q-DNS and RANS-alpha simulations even though the later method imposed a significant underestimation of shear rate and u_{rms}/η.

Variation of shear rate versus TDR/TKE, as shown in Figure 3(b), revealed two envelopes which are partly similar. The top envelope was found to contain computational cells on solid boundaries and in structures that exists in the core flow, as shown in Figure 3. It was found that the top envelope was related to regions of small u_{rms}/η which can be separated from the bottom envelope by u_{rms}/η <400 s^{-1}. Results of this structure separation in the flow filed is shown in Figure 4. This figure also shows a fine resolution display of these Structure obtained through adjusting the threshold of Q-criterion on the course resolution.

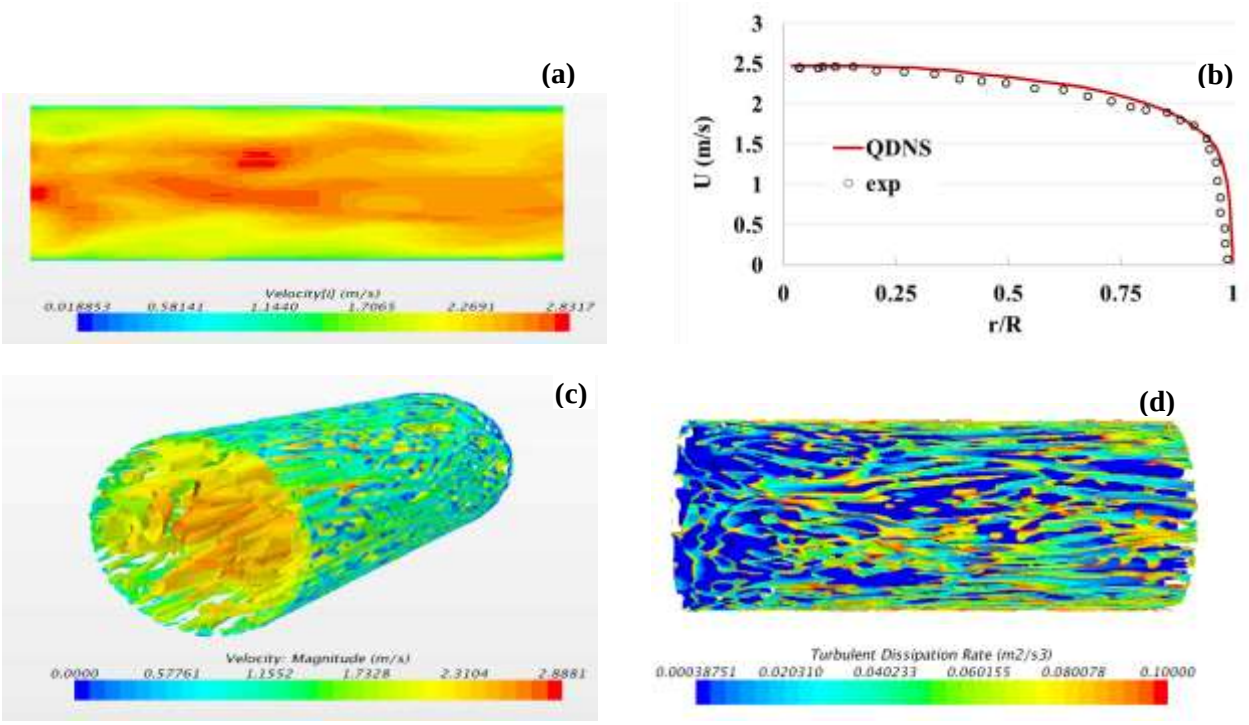

Fig. 2. Velocity and flow structures colored by velocity magnitude and TDR, Q-DNS simulation for Re = 25300.

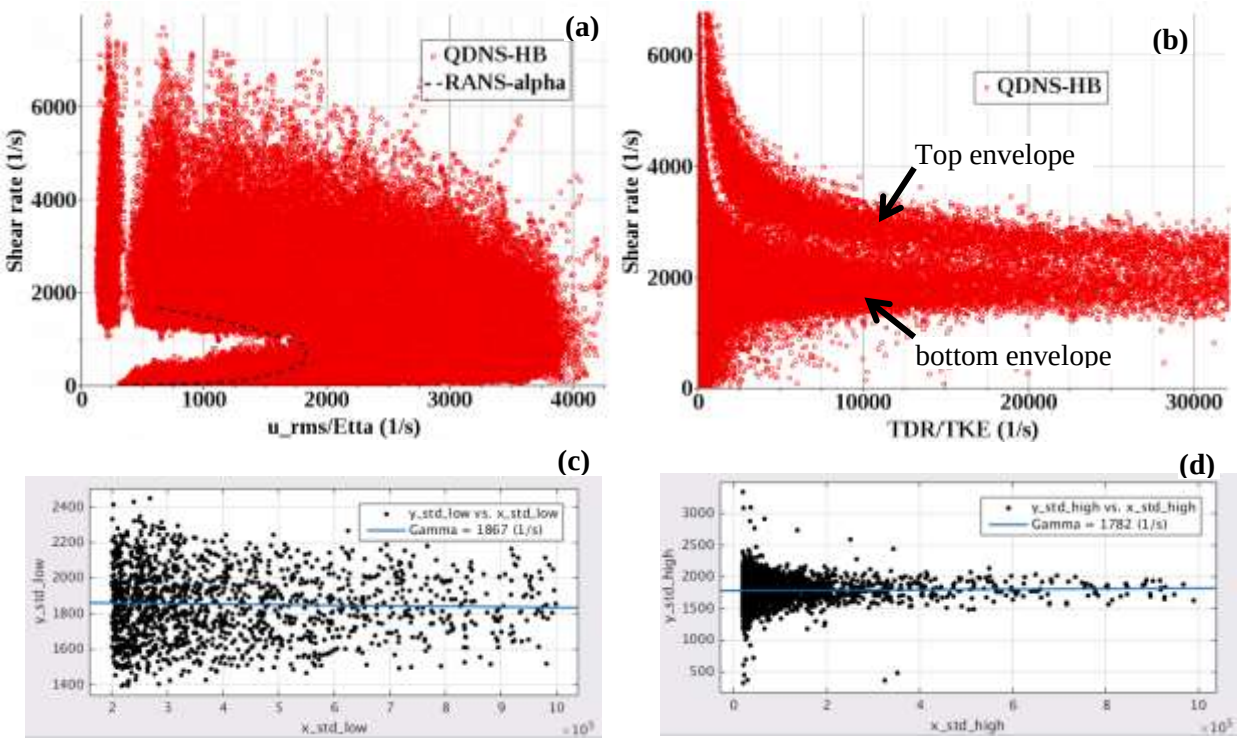

Fig. 3. Study of shear rate dependency on u_{rms}/η and TDR/TKE, Q-DNS simulation for Re = 25300.

Another observation from Figure 3(b) is that both top and bottom envelopes show reductions of shear rate with an increase of TDR/TKE. However, a region of almost constant shear rate was found in small values of TDR/TKE for the bottom envelope. Since more attention is given to higher values of the dissipation rate, trends of the variation is of major importance in higher values of TDR/TKE. A regression analysis was performed in Matlab, as shown in Figure 3(c-d), and values of 1867(1/s) and 1782 (1/s), were obtained for top and bottom envelopes, respectively.

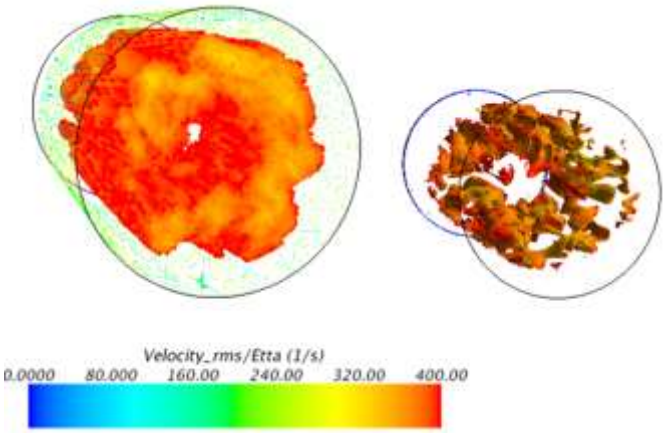

Fig. 4. Structures Found in Core Flow Which Belong to Top Envelope in Figure 3(b).

An algorithm was developed that used the converged shear rate values obtained previously in RANS-HB simulation. In this algorithm, distinction between converged values is based on values of u_{rms}/η for each cell in RANS-HB simulations. Equation 4 shows the model that was used for alteration of shear rate in RANS-HB simulation:

$$\Upsilon = \begin{cases} 1867\ (1/s) & \frac{u_{rms}}{\eta} \le \frac{u_{rms}}{\eta}\_THS \ \ \& \ \ \varepsilon_{HB} > \varepsilon\_THS \\ 1782\ (1/s) & \frac{u_{rms}}{\eta} > \frac{u_{rms}}{\eta}\_THS \ \ \& \ \ \varepsilon_{HB} > \varepsilon\_THS \\ \Upsilon_{HB} & \varepsilon_{HB} \le \varepsilon\_THS \end{cases} \qquad \text{(Eq. 4)}$$

In this model, index HB refers to simulation with HB viscosity model. Υ_{HB} is unaltered shear rate which is obtained directly from velocity field, and parameters ε-THS and u_{rms}/η _THS are defined as thresholds for the dissipation rate and u_{rms}/η, respectively. We set the ε-THS to an extremely small number to enter the entire dissipation range into modifications. Sensitivity of the model can be further reduced by increasing the ε-THS values. The value of u_{rms}/η _THS was obtained from Q-DNS, as discussed earlier, and was set to 400 s^{-1}. The shear rate obtained from the above model is then supplied to the HB viscosity model, which is defined by Equation 5.

$$\mu = \frac{\tau_\gamma}{\gamma} + k\,\gamma^{(n-1)} \qquad \text{(Eq. 5)}$$

Application of the proposed shear modification model was tested in a RANS-HB simulation of flow with Re = 25300. Results of this implementation is shown in Figure 5 and results match the profile obtained from RANS-alpha method, which is less than 2 percent different from Q-DNS-HB's results. This result shows successful implementation of the proposed shear rate modification.

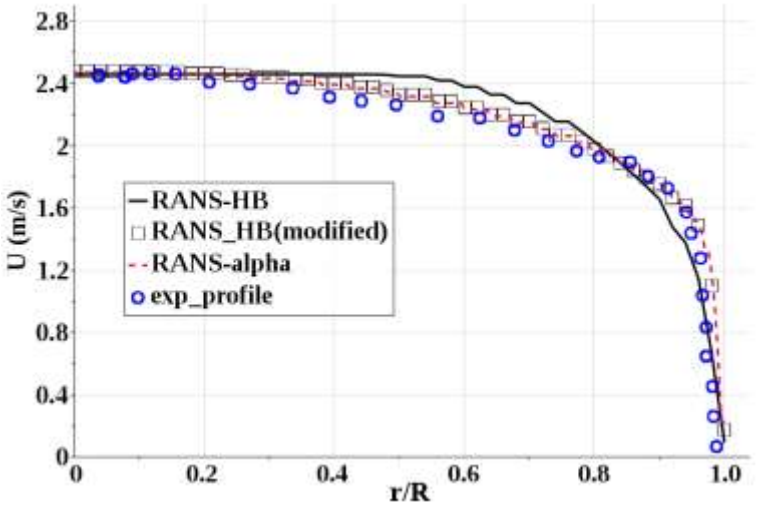

Fig. 5. Axial Velocity for Modified RANS-HB and Other RANS Simulations.

DISCUSSION AND CONCLUSION

In previous sections, we presented a method to obtain modified shear rate values based on dissipative length and velocity scales in a turbulent flow. It was observed from our Q-DNS simulation of fully turbulent flow (Re = 25300) that the shear rate converged to constant values in high ε/k values depending on values of u_{rms}/η, which represents velocity scale over length scales in dissipative structures. It was shown that for certain regions of flow (confined between axis and wall of the pipe, where values of u_{rms}/η were less than 400 s^{-1}) the shear rate converged to 1867 s^{-1}. It was also observed that the trend of shear rate reduction towards constant values was initially non-linear and this trend could be considered for a correlation. Though, due to the non-linearity of variations, a violation of consistency between units of shear rate and the resulting correlation will occur. This opens an avenue for use of non-dimensional parameters to obtain a linear relationship that maintains consistency between units. Similar variations of shear rate were observed for u_{rms}/η larger than 400 s^{-1}, provided that small values of TDR/TKE are ignored. In this paper, higher relative dissipation rates were considered for their significantly higher effects on shear rate. However, study of shear rate variation in small TDR/TKE values can be an important contribution.

Furthermore, comparison between RANS-alpha and Q-DNS-HB simulations shows that variations of shear rate versus u_{rms}/η were qualitatively similar, but significant underestimations were observed for the RANS-alpha method. It was shown that trends are similar for different Reynolds numbers in RANS-alpha simulations. However, averaging of scales and loss of information in RANS can be a significant factor in deviations. Similar deviations were again observed when variation of shear rate with TDR/TKE was considered. In RANS-alpha simulations, shear rate increased with increase of TDR/TKE; initially sharply and proceeding with a more gradual increase. However, no reduction of shear rate was observed for any of the Reynolds numbers. For this reason, extraction of correlations from the RANS-alpha method based on turbulent quantities is not recommended. Thus, an algorithm for shear modification was developed based on our Q-DNS simulation results and was implemented in our RANS-HB simulations. Shear alterations resulted in significant improvement of accuracy over most of the range of r/R. Future work can focus on extending the shear dependency analysis presented in this paper to different Reynolds numbers using DNS or Quasi DNS simulations.

REFERENCES

1. S. Gokaltun, D. McDaniel, D. Roelant, 2012, Three Dimensional Simulations of Multiphase Flows Using a Lattice Boltzmann Method Suitable for High Density Ratios – 12126, WM2012 Conference, February 26- March 1 2012, Phoenix, AZ.
2. P.A. Meyer, D.E. Kurath, C.W. Stewart, 2005, Overview of the Pulse Jet Mixer Non-Newtonian Scaled Test Program, PNWD-3677, WTP-RPT-127 Rev. 0.
3. D.R. Rector, 2016, ParaFlow Modeling of DST Mixing, DR Rector, PNNL-SA-100059, PowerPoint presentation.
4. M.P. Escudier, F. Presti, 1996, Pipe Flow of a Thixotropic Liquid, J. Non-Newtonian Fluid Mech., volume 62, PP. 291-306.
5. M.P. Escudier, R.J. Poole, F. Presti, C. Dales, C. Nouar, C. Desaubry, L. Graham, L. Pullum, 2005, Observations of Asymmetrical Flow Behaviour in Transitional Pipe Flow of Yield-Stress and Other Shear-Thinning Liquids, Journal of Non-Newtonian Fluid Mechanics, Volume 127, pp 143–155.
6. J. Peltier, A. Rizhakov, B. Rosendall, Inkson N., Lo S., 2015, Evaluation of RANS Modeling of Non-Newtonian Bingham Fluids in the Turbulence Regime Using STAR-CCM+®, Advanced Simulation & Analysis, BecthelNuclear, Security & Environmental, Cd-adapcoTM , Conference: STAR Global Conference 2015.
7. Bingham E.C., Fluidity and Plasticity, McGRAW-Hill Inc., 1922.
8. Herschel W.H., Bulkley R., 1926, Kolloid-Zeitschrift, Volume 39, Issue 4, pp 291–300, doi:10.1007/BF01432034.

9. Wilson, K.C., Thomas A.D., 1985, A New Analysis of the Turbulent Flow of Non-Newtonian.
10. Toms B.A.,1948, Some Observations on the Flow of Linear Polymer Solution through Straight Tubes at Large Reynolds Number, Proceedings of 1st Conference on Rheology, Vol.2, North Holland, Amsterdam, p135.
11. L.C.F. Andrade, J.A. Petronílio, A. deManeschy C.E., A. de Cruz D.O., 2007, The Carreau-Yasuda Fluids: a Skin Friction Equation for Turbulent Flow in Pipes and Kolmogorov Dissipative Scales, Journal of the Brazilian Society of Mechanical Science and Engineering, Vol. 29, Issue 2, p163.
12. R.J. Soto, V.L. Shah, 1976, Entrance Flow of a Yield-Power Law Fluid, Journal of Applied Science Research, Volume 32.
13. A. Bartosik, 2010, Application of Rheological Models in Prediction of Turbulent Slurry Flow, Flow Turbulence, and Combustion, Volume 84, pp 277–293.
14. A.A. Gavrilov, V.Y. Rudyak, 2014, A Model of Averaged Molecular Viscosity for Turbulent Flow of Non-Newtonian Fluids, Journal of Siberian Federal University, Journal of Mathematics & Physics, Voulem 7, Issue 1, pp 46–57.
15. A.A. Baharanchi, M. Edrei, S. Gokulton, D. McDaniel, 2016, Improving the Accuracy of Computational Fluid Dynamics Simulations of Nuclear Waste Mixing using Direct Numerical Simulations – WM2016 Conference, Phoenix, AZ, 16260.
16. A. Shams, F. Roelofs, E.J.M. Komen, B. Baglietto, 2012, Optimization of Pebble Bed Configuration for Quasi-Direct Numerical Simulations, Nuclear Engineering and Design 242 (2012) 331– 340.
17. A. Shams, F. Roelofs, E.J.M Komen, B. Baglietto, 2013, Quasi-Direct Numerical Simulations of a pebble bed configuration, Part-2: Temperature field analysis, Nuclear Engineering and Design 263 (2013) 490– 499.
18. A. Shams, F. Roelofs, E.J.M. Komen, B. Baglietto, 2013, Quasi-Direct Numerical Simulations of a pebble bed configuration, Part-1: Flow (velocity) field analysis, Nuclear Engineering and Design 263 (2013) 473– 489.
19. E. Komen, A. Shams, L. Camilo, B. Koren, 2014, Quasi-DNS Capabilities of OpenFOAM for Differen mesh types, Computers & Fluids 96 (2014) 87–104.